J Fluoresc (2015) 25:603–611
DOI 10.1007/s10895-015-1541-1

ORIGINAL PAPER

Two Different Emission-Wavelength Fluorescent Probes for Aluminum Ion based on Tunable Fluorophores in Aqueous Media

Yanxia Li · Zengchen Liu · Wenping Zhu · Hao Fu · Yongjie Ding · Jianping Xie · Weijie Yang · Lili Li · Chao Cheng

Received: 30 November 2014 / Accepted: 23 February 2015 / Published online: 18 March 2015

Abstract Two simply and highly selective aluminium ion fluorescent probes based on 4-aminoantipyrine derivate have been successfully synthesized and systemically characterized, The investigation of absorption and emission spectra revealed that the compounds exhibited highly selective fluorescence behaviours toward Al^{3+} in aqueous media and showed differential fluorescent emission peaks corresponding to blue and green. which resulted from different fluorophores, and the fluorescence process is attributed to the Photoinduced Electron Transfer (PET) mechanism, In addition, the association constants between sensors **L1** and **L2** with aluminum ion are 1.58×10^6 M^{-1} and 8.72×10^6 M^{-1}, respectively, which were obtained by fluorescent titration experiments. Moreover, the binding site of sensors with Al^{3+} were determined by ^{1}HNMR titration experiments.

Keywords Fluorescent sensor · Naphthalene derivate · Water-solubility, Aluminium ion · Selectivity, PET process

Introduction

Aluminium is the third most abundant metallic element in the earth, which accounts for 7.45 % of the total of the earth's crust [1, 2]. Despite being a non-essential element in living organism, the detection of aluminum is very necessary and of great interest due to its potential toxicity and extensive application in packing materials, clinical drugs, deodorants and food additives et al. [3–7]. Aluminium has been proved to be a neurotoxin for a long time, and the abnormal content of aluminium can cause many health hazards such as alzheimer's disease, osteomalacia and the risk of breast cancer, meanwhile, it can damage the brains and kidneys [8–11]. Some relevant aluminium compounds are frequently utilized as pharmaceutical drugs in the human body, for example, the drug aspirin containing aluminium glycinate is commonly used as an analgesic, the antacids is a kind drugs of regulating pH in organism. Additionally, the WHO (World Health Organization) prescribed the average human intake of aluminum as around 3–10 mg day^{-1} with a weekly dietary intake of 7 mg kg-1 body weight. Meanwhile, as far as can be determined, 40 % of soil acidity arises from aluminum toxicity, furthermore, high concentration of aluminium in ecosystem is toxic to plant, fish, algae and other species, and can enter into human body along with biocycle to cause other relevant diseases [12–16].

Because of the potential harm of aluminium on environment and human health, the researchers attempted to explore more efficient analytical methods toward aluminium [17–19]. In recent years, compared with the traditional detection methods (graphite furnace atomic absorption spectrometry and inductively coupled plasma atomic emission spectrometry), fluorescent probe has been regarded as an effective method for tracing relevant metal ions and shows its special advantages [20–23]. As already reported, some fluorescent probes toward aluminium ion derived from coumarin, 8-hydroxyquinoline and rhodamine et al. have been reported, but some metal ions (Cu^{2+}, Cd^{2+}, Zn^{2+} et al.) can interfere with the detection of aluminium ion [24–26]. Additionally,

Y. Li · Z. Liu (✉) · W. Zhu · H. Fu · Y. Ding · J. Xie · W. Yang · C. Cheng
College of Chemistry and Chemical Engineering, Zhoukou Normal University, Zhoukou 466001, People's Republic of China
e-mail: liuzch07@lzu.edu.cn

Z. Liu · L. Li
The Key Laboratory of Rare Earth Functional Materials and Applications, Zhoukou Normal University, Zhoukou 466001, People's Republic of China

aluminium ion exists in aqueous environment in general and most of the reported fluorescent probes of Al^{3+} have weak water-solubility, which limits its application prospect, so the design of highly selective and sensitive probe of Al^{3+} is very necessary for its practical application. Based on the features, there is a extra demand for the design and synthesis of fluorescent probe for detecting aluminium ion in natural environment and living organism.

In the process of the development of fluorescent sensors, 4-diethylaminobenzaldehyde and naphthalene moiety have been proved as ideal fluorophores and some correlative derivates have been synthesized as effective fluorescent probes in determination of some cations [27–29]. Especially over the years, some highly selective and sensitive fluorescent probes for Al^{3+} from their derivates have been reported, which exhibit high signal response toward Al^{3+}. 4-aminoantipyrine is an important organic compound which can be acted as a color development reagent and chelating group which is applied in coordination chemistry [30, 31]. But to date, the study of fluorescent probes based on 4-aminoantipyrine derivates are scare.

In continuation of our work on biological and environmental important cations probes, herein, two fluorescent probes based on 4-aminoantipyrine have been exploited, the strong binding property between fluorescent probe and Al^{3+} leads to high selectivity and sensitivity over competing metal ions. According to the spectral analysis, the two fluorescent probes exhibited different emission wavelengths, the typically spectral characters, which can be used combinedly to detect Al^{3+}, will enhance the accuracy and sensitivity. The spectra properties of probes for Al^{3+} improve the prospects in environment monitoring and biological analysis.

Experimental

Instrument and Reagents

^{1}HNMR spectra were recorded on a Bruker Avance III 400 spectrometer with TMS as an internal standard. The melting points of the compound were determined on a Beijing XT4-100X microscopic melting point apparatus. The UV–vis spectra were recorded on a Perkin-Elmer Lambda-35 UV–vis spectrophotometer. Fluorescence spectra were obtained on a Cary Eclipse spectrophotometer at room temperature.

Naphthol aldehyde, 4-aminoantipyrine and 4-diethylamino benzaldehyde were purchased from aladdin reagent corporation. All the chemicals were of reagent grade and were used without further purification.

All spectroscopic measurements were performed in Ethanol-HEPES buffer solution (99:1, pH=7.0).

Stock solutions (1.0×10^{-3} M) of metal ions (metal chloride) were prepared in two-distilled water. The stock solution of sensors (1.0×10^{-3} M) was prepared in two-distilled water. In titration experiments, each time a 20 μL solution of sensor (1.0×10^{-3} M) was filled in a quartz optical cell of 1 cm optical path length. Then equal amount of Al^{3+} stock solution (5 μL) was added to the compound solution with micro-pippet. Spectral data was recorded at 1 min after addition. In selectivity experiment, the test samples were prepared by placing appropriate amounts of metal ion stock into 3 mL solution of sensor (6.67×10^{-6} M). For fluorescence measurements, the excitation wavelength is at 360 nm.

The binding constant between sensor and Al^{3+} was calculated by the linear Benesi-Hildebrand expression [32, 33].

$$I_0/(I-I_0) = I_0/[\mathbf{L}] + I_0/[\mathbf{L}].Ks.[M]$$

Where I is the change in the fluorescence intensity at 450 and 485 nm, Ks is the stability constant, and [L] and [M] are the concentration of **L1**, **L2** and Al^{3+}, respectively. I_0 is the fluorescence intensity of **L1** and **L2** in the absence of Al^{3+}. On the basis of the plot of 1 / (I-I_0) versus 1 / [Al^{3+}], the stability constant can be obtained.

Synthesis of Compounds 4-diethylaminobenzaldehyde-4-aminoantipyrine Schiff-Base (L1) and Naphthol aldehyde-4-aminoantipyrine Schiff-Base (L2)

The two compounds were synthesized by the reported methods [34, 35]. The synthetic route of 4-diethylaminobenzaldehyde-4-aminoantipyrine schiff-base was shown in Scheme 1. An ethanol solution (10 mL) of 4-aminoantipyrine (1 mmol, 0.2032 g) was added to another ethanol (10 mL) containing 4-diethylaminobenzaldehyde (1 mmol, 0.1932 g), Then the solution was reflux for 4 h and cooled to room temperature. The mixture was filtered and dried under vacuum. Recrystallization from C_2H_5OH/H_2O (V:V=1:1) gave the target product 4-diethylaminobenzaldehyde-4-aminoantipyrine schiff-base (**L1**), which was dried under vacuum. Yield, 86 %. m.p.: 236–238 °C. ^{1}HNMR (DMSO–d_6 400 MHz): δ 13.361 (1H, s, $-O^2-$H), δ 9.505 (1H, s, $-C^1-$H), δ 7.541–7.577 (2H, m, $-C^{11,13}-$H), δ 7.399–7.418 (3H, d, $-C^{10,12,14}-$H), δ 7.175–7.196 (1H, d, $-C^6-$H), δ 6.277–6.296 (1H, d, $-C^7-$H), δ 6.083 (1H, s, $-C^3-$H), δ 3.153 (3H, s, $-C^9-$H), δ 3.532 (4H, m, $-C^{4,4'}-$H), δ 2.372 (3H, s, $-C^8-$H), δ 1.123–1.155 (6H, m, $-C^{5,5'}-$H).

Naphthol aldehyde-4-aminoantipyrine schiff-base (L2) was synthesized by the same route with **L1** (Scheme 1), Yield, 85 %. m.p.: 258–260 °C. ^{1}HNMR (DMSO–d_6 400 MHz): δ 15.001 (1H, s, $-O^2-$H), δ 10.864 (1H, s, $-C^1-$H), δ 8.102–8.123 (1H, d, $-C^3-$H), δ 7.975–8.102 (1H, d, $-C^{11}-$H),, δ 7.900–7.902 (1H, d, $-C^{15}-$H), δ 7.571–7.624 (3H, m, $-C^{12,13,14}-$H), δ 7.399–7.457 (4H, m, $-C^{5,6,7,8}-$H), δ 7.199–-7.222 (1H, d, $-C^4-$H), δ 3.268 (3H, s, $-C^{10}-$H), δ 2.472 (3H, s, $-C^9-$H).

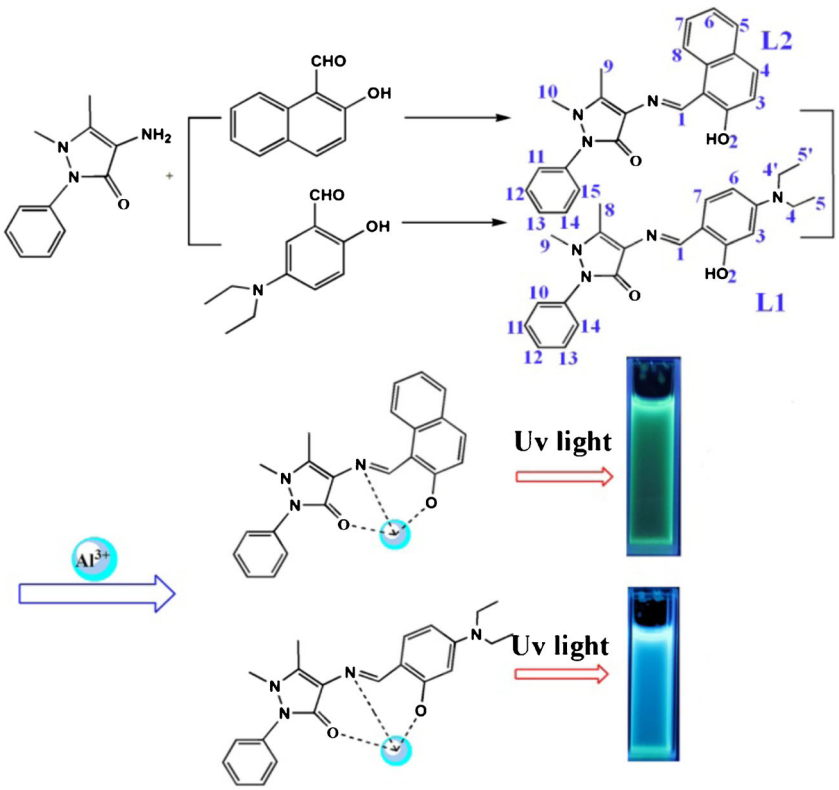

Scheme 1 The structures and synthetic route of corresponding compounds 4-diethylaminobenzaldehyde-4-aminoantipyrine schiff-base (**L1**) and naphthol aldehyde-4-aminoantipyrine schiff-base (**L2**)

Investigation of UV–vis Spectra between Probes L1, L2 and Al^{3+}

Figure 1a and b showed the change in the UV–vis spectra of sensors **L1**, **L2** (6.67×10^{-6} M) with addition of Al^{3+} (0–4 equiv.) in Ethanol-HEPES media. The compounds **L1** and **L2** exhibited obvious maximum absorption. With the gradual addition of Al^{3+} in Ethanol-HEPES media, the UV–vis spectra from **L1** and **L2** showed significant changes. Figure 1a showed the UV–vis titration spectrum changes of **L1** with Al^{3+} in Ethanol-HEPES media, The absorption bands at 375 and 380 nm disappeared with the generation of new bands at 350 and 430 nm, which illustrated that there was intense interaction between **L1** and Al^{3+}. As listed in Fig. 1b. UV–vis titration spectrum of **L2** with Al^{3+} showed the absorption band at 375 nm exhibited gradual decrease with red shift of absorption peak in the range. Simultaneously, The isoabsorptive point at 400 nm proved the form of coordinative compound between **L2** and $\mathbf{Al^{3+}}$. But it needed to be demonstrated further by fluorescence measurement.

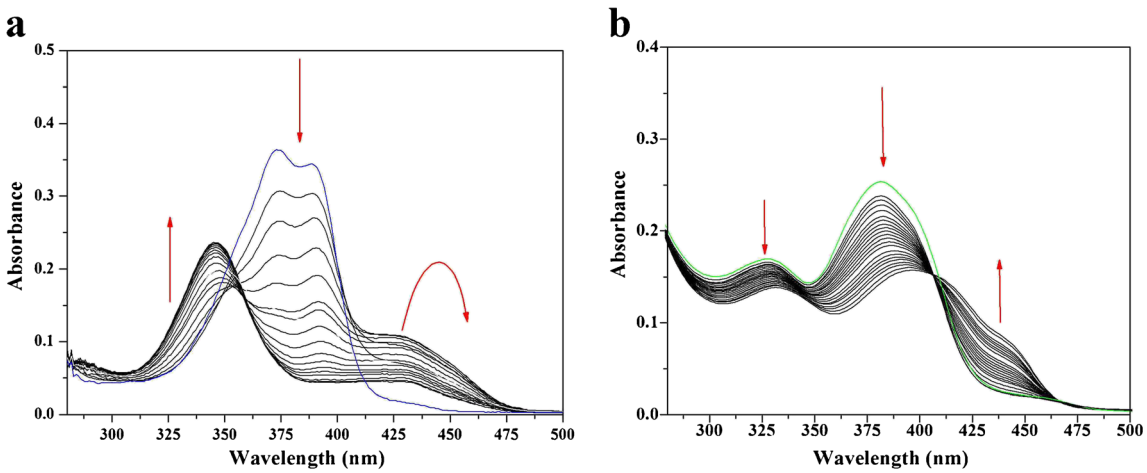

Fig. 1 The interactive UV–vis spectra of **L1**, **L2** with Al^{3+} in Ethanol-HEPES media

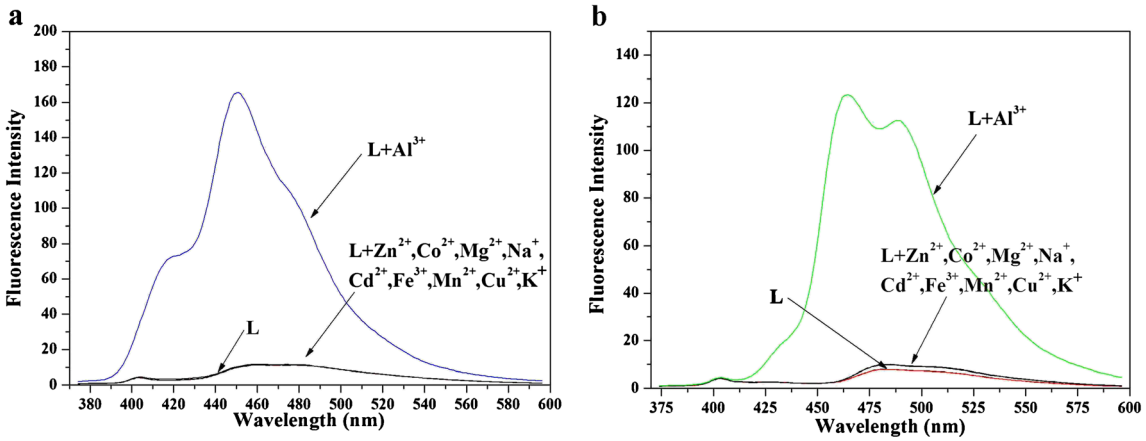

Fig. 2 The fluorescence spectra changes of sensors **L1** (**a**) and **L2** (**b**) upon addition of various metal ions in Ethanol-HEPES media

Investigation of Fluorescence Spectrum between Sensors L1, L2 and Al^{3+}

The fluorescence selective activities of **L1** and **L2** toward various metal ions (Na^{+}, Cu^{2+}, Zn^{2+}, Co^{2+}, Cr^{3+}, Cd^{2+}, Mn^{2+}, Fe^{3+}, Al^{3+}) were evaluated in Ethanol-HEPES solution. The fluorescence selective spectra of **L1** and **L2** with metal ions were validated by the excitation at 360 nm. As shown in Fig. 2a, in Ethanol-HEPES buffer solution, the sensor **L1** exhibited almost no fluorescence at 450 nm. Upon gradual addition of various metal ions, only Al^{3+} could cause a significant fluorescence enhancement from **L1** (16 fold increasing), very few of fluorescence changes were observed in the presence of other metal ions. The fluorescence behaviors showed

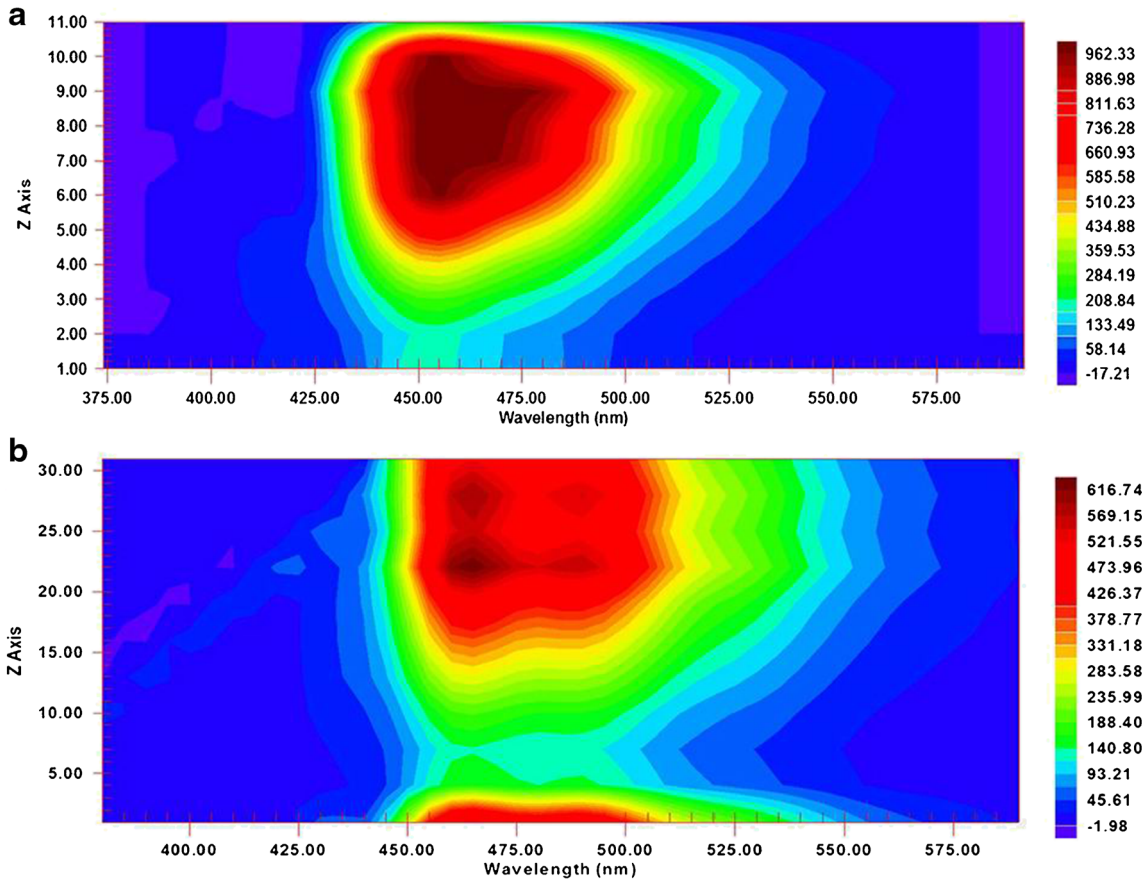

Fig. 3 The three-dimensional (3D) fluorescence spectra of sensors **L1** (**a**) and **L2** (**b**) upon addition of Al^{3+} in Ethanol-HEPES media

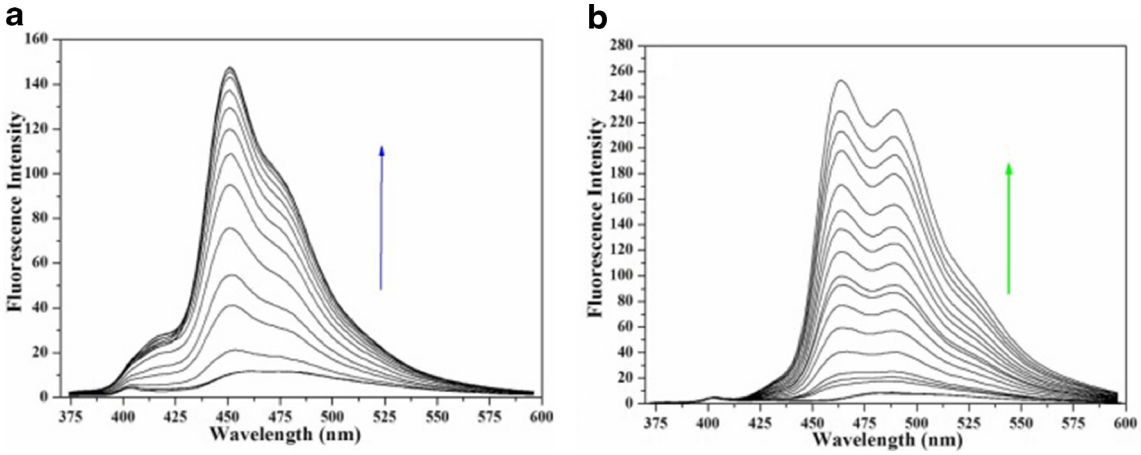

Fig. 4 The fluorescence titration spectra of sensors **L1** (**a**) and **L2** (**b**) upon addition of Al^{3+} in Ethanol-HEPES media

that sensor **L1** exhibited high fluorescent selectivity toward Al^{3+} in aqueous environment. Meanwhile, to illustrate the high selectivity of **L2** toward Al^{3+}, the fluorescence spectrum under the same experimental conditions was also tested. As shown in Fig. 2b, **L2** showed obvious emission at 460 and 485 nm upon addition of Al^{3+} in comparison with other metal ions. In addition, the 3D fluorescence spectra (Fig. 3) were also tested to indicate the different emission bands. It demonstrated the interaction of **L1** with Al^{3+} lead to one emission band at 450 nm, while the interaction between **L2** and Al^{3+} exhibited two obvious bands at 460 and 485 nm. By compare with the fluorescence properties of **L1** and **L2** toward Al^{3+}, the emissive wavelength were distinctly discriminating. The emission of **L1** treated with Al^{3+} was limited in the range of blue light, while the fluorescence of L2 with Al^{3+} was green. And they could be illustrated intuitively by the fluorescence images under UV light (Scheme 1 insert).

The fluorescence titration experiments between **L1** and **L2** with Al^{3+} was also conducted (Fig. 4a and b). Because It could illuminate directly the interactive fluorescence activities between sensors with Al^{3+}. Additionally, the binding constant of sensors and Al^{3+} could be calculated by fluorescence titration spectra, which could explain quantificationally the combining capacity of sensors and Al^{3+}. As shown in Fig. 4, the fluorescence titration spectrum showed a gradually enhanced fluorescence with addition of Al^{3+}. By Benesi-Hildebrand expression (Fig. 5), the binding constants **L1** and **L2** with $\mathbf{Al^{3+}}$ were estimated to be 1.58×10^6 M^{-1} and 8.72×10^6 M^{-1}, respectively, which demonstrated that **L2** exhibited stronger binding affinity with $\mathbf{Al^{3+}}$ than **L1**. Meanwhile, the binding properties were proved qualitatively by molecular exchange experiment (Fig. 6). Adding **L2** to the solution of **L1**-Al^{3+}, the fluorescence changed from blue to green along with the change of fluorescence emission wavelength, but the reversible exchange process was impracticable. The fluorescence transition properties could be used to detect and analysis Al^{3+} accurately in environment and organism.

Furthermore, to validate the high selectivity of **L1** and **L2** toward Al^{3+}, the fluorescence competitive experiments of other various metal ions were also investigated. Equivalent Al^{3+}

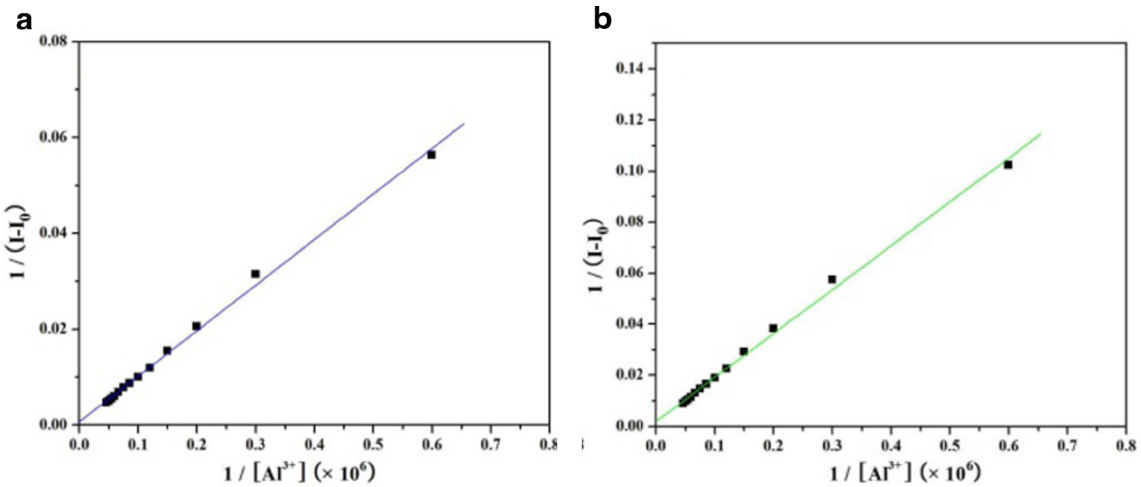

Fig. 5 The Benesi-Hildebrand expressions of sensors **L1** (**a**) and **L2** (**b**) upon addition of Al^{3+} in Ethanol-HEPES media

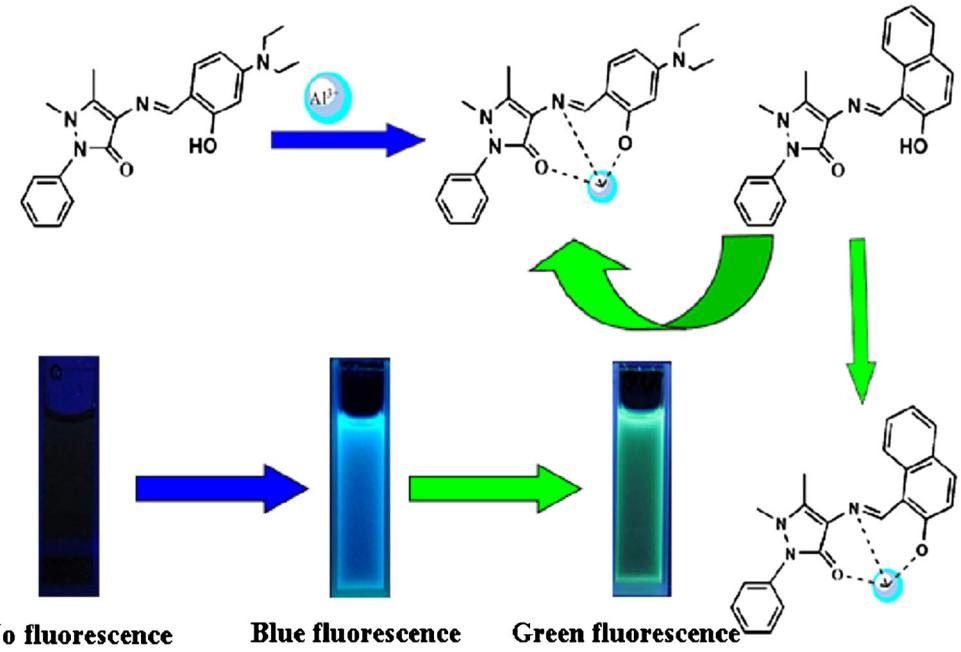

Fig. 6 The fluorescence reversible process of sensors **L1** (**a**) and **L2** (**b**) in Ethanol-HEPES media

was added to the aqueous solution of **L1** and **L2** (6.67×10^{-6} M), then equivalent amount of other metal ions were also added into the solution. Their fluorescence intensities were recorded, respectively. The histogram of fluorescence changes were listed in Fig. 7. As shown in Fig. 7a and b, the fluorescence emission intensity of **L**-Al^{3+} solution containing other metal ions (Na^+, Cu^{2+}, Zn^{2+}, Co^{2+}, Cr^{3+}, Cd^{2+}, Mn^{2+}, Fe^{3+}) showed no significant variation in comparison with the fluorescence intensity of **L**-Al^{3+} solution. All the results indicated that the **L1** and **L2** could be used as highly selective fluorescent sensors for Al^{3+} in aqueous environment.

The Job plot (Fig. 8) was described to determine the accurate coordination stoichiometry of **L**-$\mathbf{Al^{3+}}$ complex. The fluorescence emission was measured for each sample in Ethanol-HEPES solution with the excitation wavelength at 360 nm. The total concentration of sensors and $\mathbf{Al^{3+}}$ (1.0×10^{-5} M) was fixed, in the experimental process, the concentration ratio of **L** and Al^{3+} changed correspondingly. In Fig. 8, the plot of fluorescence intensity versus $[Al^{3+}]/[Al^{3+}+\mathbf{L}]$ showed the maximum fluorescence value is 0.46 and 0.50, respectively, which indicated that the 1:1 coordination stoichiometry between **L1**, **L2** and Al^{3+}.

Investigation of ^{1}HNMR Titration Spectrum, Fluorescence Emission Mechanism and Detection Limit

The stoichiometry of **L** and Al^{3+} had been calculated by Job plot, but the coordinative sites of sensor **L** and Al^{3+} was not

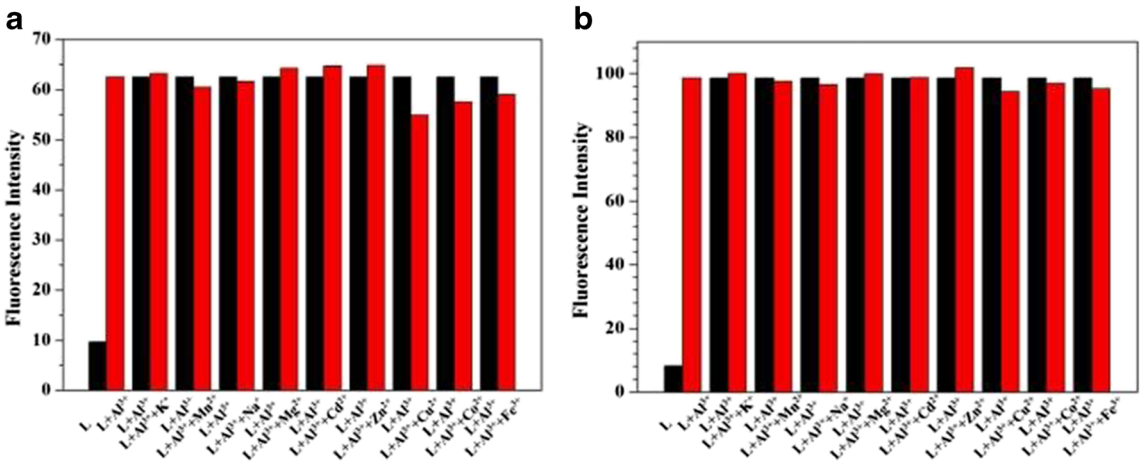

Fig. 7 The selectivity of **L1** and **L2** for $\mathbf{Al^{3+}}$ in the presence of other metal ions ($\mathbf{Na^+}$, $\mathbf{Cu^{2+}}$, $\mathbf{Zn^{2+}}$, $\mathbf{Co^{2+}}$, $\mathbf{Cr^{3+}}$, $\mathbf{Cd^{2+}}$, $\mathbf{Mn^{2+}}$, $\mathbf{Fe^{3+}}$, $\mathbf{Al^{3+}}$) in Ethanol-HEPES media (pH=7.0). Excitation at 320 nm. The response is normalized with respect to background fluorescence of the free **L** (1.0×10^{-5} M). $\mathbf{Al^{3+}}$ (1.0×10^{-5} M) is added at first. Then other metal ions were added (1.0×10^{-5} M)

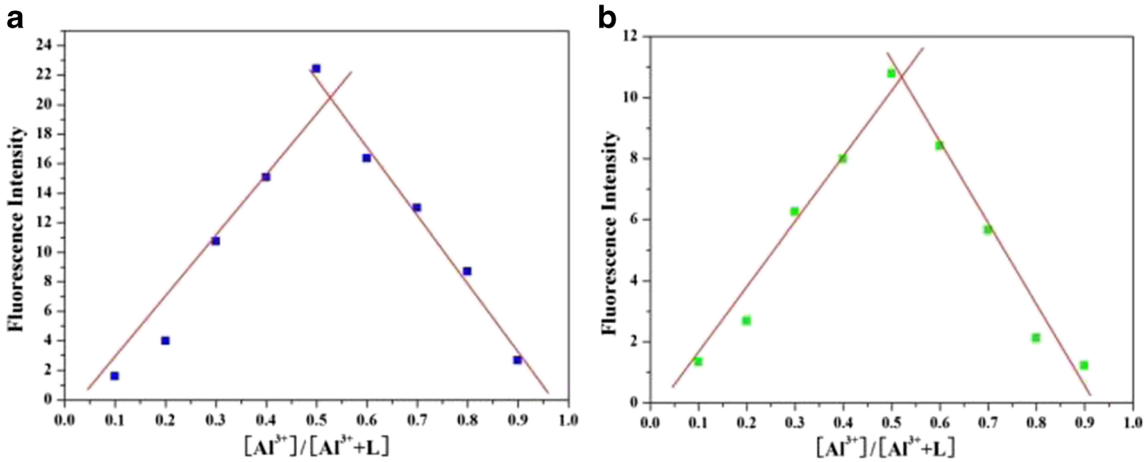

Fig. 8 Job's plot according to the method for continuous variations, indicating the 1:1 stoichiometry for **L1**-Al^{3+} and **L2**- Al^{3+} (the total concentration of **L** and Al^{3+} is 1.0×10^{-5} M). (λex=360 nm, Slit: excitation/emission=5/5)

sure, so to confirm the coordinative sites, ^{1}HNMR titration spectrum of **L** with Al^{3+} was tested. Figure 9 showed the ^{1}HNMR spectroscopy of **L1** and **L2** in the absence and presence of Al^{3+}. As shown in Fig. 9, the ^{1}HNMR titration spectra showed same features. the coordination of sensor **L** with Al^{3+} lead to the departure of H ion from hydroxyl groups of sensor **L1** and **L2**. By the information from H-chemical shifts, we could primarily confirm that one important coordinative cite of **L1** and **L2** for Al^{3+} was from hydroxyl group, which is similar to the reported fluorescent sensor [29, 36–38]. In addition, the supposed fluorescence emission mechanism was listed in Fig. 10. Al^{3+} played the role of electron acceptor, before sensor **L** coordinated with Al^{3+}, **L** transfered the electron (non-bonding electron pair from nitrogen atom) to the fluorophores (4-diethylamine benzyl and naphthyl ring), which caused fluorescence quenching. After **L1** and **L2** coordinated with Al^{3+}, the PET (Photoinduced Electron Transfer) process from the receptor (nitrogen atom) to the fuorophores (4-diethylamine benzyl and naphthyl rings) was blocked and the fluorescence switched "ON". To evaluate the sensitivity of sensor **L1** and **L2** with Al^{3+}, the detection limit in recognizing Al^{3+} was also tested using fluorescence spectra. The

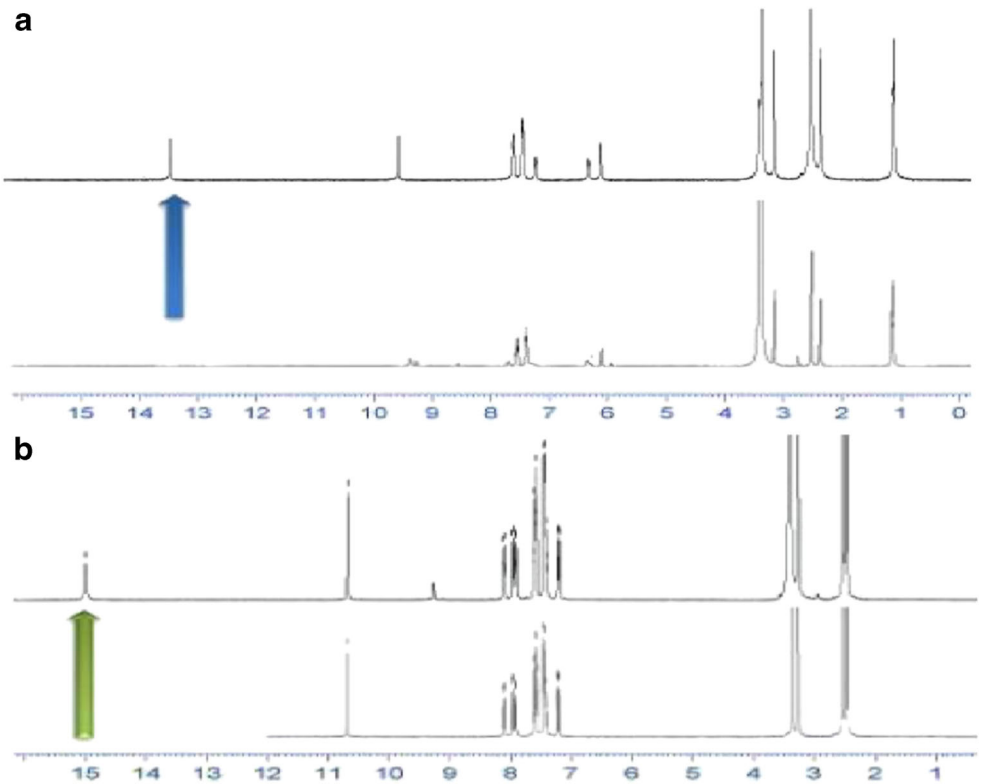

Fig. 9 The ^{1}HNMR titration experiment of **L1** (**a**) and **L2** (**b**) with Al^{3+} in d^6-DMSO solution

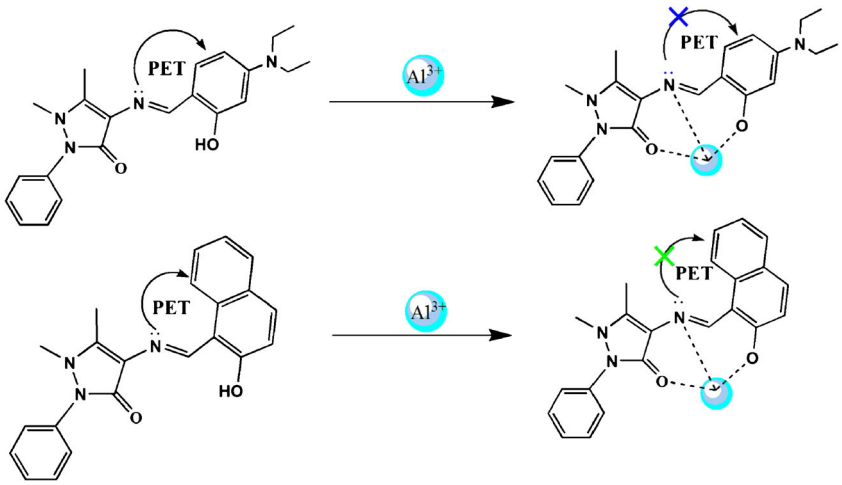

Fig. 10 The proposed fluorescence emission mechanism of **L1**, **L2** with Al^{3+}

fluorescence titration experiment of **L** with Al^{3+} demonstrated the detection of Al^{3+} in aqueous media was at the magnitude level of 1.0×10^{-7} M, which was relatively sensitive.

Conclusion

In summary, we have presented two simple 4-aminoantipyrine derived fluorescent chemosensors for Al^{3+}. They exhibits high selectivity and sensitivity toward Al^{3+} over various metal ions in aqueous media. The interaction of **L1** and **L2** with Al^{3+} lead to intense blue and green fluorescence, respectively. Moreover, according to the spectrum investigation, the 1:1 stiochiometry between sensors and Al^{3+} are obtained. In addition, there is a higher association constant between **L2** and Al^{3+}, which exhibits competitive advantage comparing with **L1**. And the coordinative sites of sensors with Al^{3+} are confirmed by ^{1}HNMR titration spectrum. The fluorescence properties of sensors **L1** and **L2** with Al^{3+} in aqueous media enhance their potential application value of the monitoring and tracking of aluminum ions in biological system and environment.

Acknowledgments This work is supported by the Research Start Funds Sponsored Program of Zhoukou Normal University (zksybscx201201, ZKNUB2013002, zksybscx201106), Science and Technology Research Projects of the Education Department Henan Province (14B150037), The Henan Province Foundation and Advanced Technology Research Program (142300410348, 132300410481), College of Chemistry and Chemical Engineering Science and Technology Innovation Fund (HYDC201408), The National Natural Science Foundation of China (21477167).

References

1. Godbold DL, Fitz E, Huttermann A (1998) Proc Natl Acad Sci U S A 85:3888
2. Miller WS, Zhuang L, Bottema J, Wittebrood AJ, Smet PD, Haszler A, Vieregge A (2000) Mater Sci Eng A 280:3
3. Sont MG, White SM, Flamm WG, Burdock GA (2001) Regul Toxicol Pharmacol 33:66
4. Berthon G (2002) Coord Chem Rev 228:319
5. Bielarczyk H, Jankowska A, Madziar B, Matecki A, Michno A, Szutowicz A (2003) Neurochem Int 42:323
6. Baylor NW, Egan W (2002) Vaccine 20:18
7. Fu Y, Jiang XJ, Zhu YY, Zhou BJ, Zang SQ, Tang MS, Zhang HY, Maka TCW (2014) Dalton Trans 43:12624
8. Perl DP, Brody AR (1980) Science 208:297
9. Becaria A, Campbell A, Bondy SC (2002) Toxicol Ind Health 18:309
10. Pierides AM, Edwards WG Jr, Cullum UX Jr, McCall JT, Ellis HA (1980) Kidney Int 18:115
11. Roskams AJ, Connor JR (1990) Proc Natl Acad Sci U S A 87:9024
12. Alvarez E, Marcos MLF, Monterroso C, Sanjurjo MJF (2005) Ecol Manag 211:227
13. Barceló J, Poschenrieder C (2002) Environ Exp Bot 48:75
14. Krejpcio Z, Wojciak RW (2002) Pol J Environ Stud 11:251
15. Flaten TP, Odegård M (1988) Food Chem Toxicol 26:959
16. Yokel RA (2000) Neurotoxicology 21:813
17. Liu ZC, Li YX, Ding YJ, Yang ZY, Wang BD, Li Y, Li TR, Lu W, Zhu WP, Xie JP, Wang CJ (2014) Sens Actuat B Chem 197:200–205
18. Mukherjee M, Pal S, Lohar S, Sen B, Sen S, Banerjee S, Banerjee S, Chattopadhyay P (2014) Analyst 139:4828
19. Lian H, Kang Y, Bi S, Arkin Y, Shao D, Li D, Chen Y, Dai L, Gan N, Tian L (2004) Talanta 62:43
20. Downard AJ, O'Sullivan B, Powell KJ (1997) Anal Chim Acta 345:5
21. Sarkar D, Pramanik A, Biswas S, Karmakar P, Kumar Mondal T (2014) RSC Adv 4:30666
22. Datta BK, Kar C, Basu A, Das G (2013) Tetrahedron Lett 54:771–774
23. Gong WT, Zhang QL, Shang L, Gao B, Ning GL (2013) Sens Actuat B Chem 177:322–326
24. Wang LY, Li HH, Cao DR (2013) Sens Actuat B Chem 181:749–755
25. Sharma S, Hundal MS, Walia A, Vanita V, Hundal G (2014) Org Biomol Chem 12:4445–4453
26. Shellaiah M, Wu YH, Lin HC (2013) Analyst 138:2931–2942
27. Sahana A, Banerjee A, Das S, Lohar S, Karak D, Sarkar B, Mukhopadhyay SK, Mukherjee AK, Das D (2013) Org Biomol Chem 9:5523–5529
28. Sen S, Mukherjee T, Basab Chattopadhyay A, Moirangthem A, Basu J, Chattopadhyay PM (2013) Analyst 137:3781–3795
29. Das S, Dutta M, Das D (2013) Anal Methods 5:6262–6285
30. Dessingou J, Tabbasum K, Mitra A, Hinge VK, Rao CP (2012) J Org Chem 77:1406–1413

31. Liu ZC, Yang ZY, Li TR, Wang BD, Li Y, Wang MF (2011) Transit Met Chem 36:489–498
32. Zhi LH, Liu J, Wang Y, Zhang W, Wang BD, Xu ZG, Yang ZY, Huo X, Li GM (2013) Nanoscale 5:1552
33. Benesi HA, Hildebrand JH (1949) J Am Chem Soc 71:2703–2707
34. Mahalingam V, Frank NC, Fronczek R, Natarajan K (2010) Polyhedron 29:3363–3371
35. Al-Khamees HA, Bayomi SM, Kandil HA, El-Tahir KEH (1990) Eur J Med Chem 25:103–106
36. Sharma H, Narang K, Singh N, Kaur N (2012) Mater Lett 84:104
37. Jiang XH, Wang BD, Yang ZY, Liu YC, Liu ZC (2011) Inorg Chem Commun 14:1224
38. Zhang X, Guo L, Wu FY, Jiang YB (2003) Org Lett 5:2667